Journal of Petroleum Science and Engineering, 9 (1993) 251–261
Elsevier Science Publishers B.V., Amsterdam

Waterflooding in a tarmat reservoir laboratory model

S.A. Abu-Khamsin, M. Ayub, M.A. Al-Marhoun and H. Menouar
Department of Petroleum Engineering, King Fahd University of Petroleum and Minerals, Dhahran, Saudi Arabia

(Received May 11, 1992; revised and accepted January 28, 1993)

ABSTRACT

The existence of natural barriers such as tar deposits in oil reservoirs can create problems in primary oil recovery as well as in the application of EOR methods. Significant reduction in oil recovery is reported from this type of reservoirs due to isolation of the oil zone from the adjacent water aquifer.

In this study, the effects of tar viscosity and thickness of a tar zone on oil recovery as well as the pressure variation and average water saturation in the tar and oil zones were studied in a tarmat reservoir laboratory model. Waterflooding experiments were conducted, whereby the three adjacent oil, tar and water zones were simulated by means of a berea composite core saturated with kerosene, a blend of asphalt and crude oil and KCl brine, respectively. In every experiment, brine was injected at a constant rate in the water zone and was forced to penetrate the tar zone to flood the oil zone.

The results show a slight decrease in oil recovery as the product of the viscosity and the thickness of the tar zone increases. An opposite and more pronounced trend was found for the average water saturation in the tar zone. The injection pressure was found to go through a maximum shortly after commencement of injection and the maximum value increased with both tar viscosity and tar zone thickness. On the other hand, the effective permeability to water was found to be smaller in tests where the product of the tar viscosity and tar zone thickness is higher. Finally, the water saturation distribution in the oil zone combined with the pressure behavior points to the development of water fingers in both tar and oil zones.

Introduction

A number of major oil reservoirs in the world, particularly in the Middle East, is documented to contain a layer of very viscous oil (tarmat) at the oil/water contact. The causes of tarmat formation are discussed extensively in the literature (Moor, 1984; Hirschberg, 1988). One of the most acceptable theories attributes tarmat formation to compositional variation in the oil column, or the segregation of asphaltenes, resulting in the variation in oil viscosity (Hirschberg, 1988). The viscosity of the tar may be 1000 times more than that of the overlaying oil. The thickness of the tarmat generally varies from place to place within a reservoir. In some reservoirs it is comparable to that of the oil zone (Al-Kaabi et al., 1988). In Ghawar oil field (world's largest), for ex-

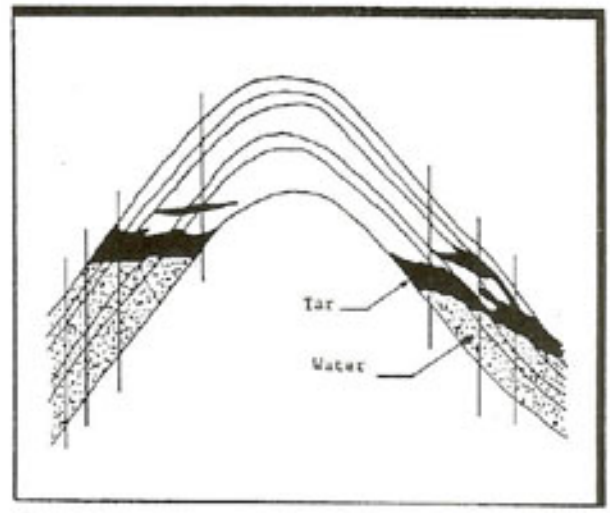

Fig. 1. A reservoir cross-section showing the tarmat, (from Bashbush et al., 1983).

ample, the tar zone extends over 25 km and reaches in certain areas up to 150 m in thickness. In this area alone, tar reserves exceed 2.3 $\times 10^8$ barrels (Osman, 1985).

In general, it is believed that the tar is immobile or partially mobile, and its extension over the aquifer can be either continuous or discontinuous. In some reservoirs, it may completely isolate the oil zone from the aquifer, hence impeding bottom water drive as depicted in Fig. 1 (Bashbush et al., 1983).

Discontinuous tarmat barriers cause a significant reduction in the vertical and horizontal permeabilities due to the tortuous path and changing contact area of the fluid flow during the depletion stage. This is believed to have adverse effects on the oil recovery and success of secondary recovery projects (Richardson et al., 1978).

Continuous tarmats may not separate the reservoir into a completely independent hydraulic unit, due to the existence of some vertical permeability, that varies according to the physical characteristics of the tar itself. Practically, tar "break down" may occur after a certain period of continuous production or injection (Osman, 1985). Excessive pressure decline in the oil zone due to production, or large pressure increase due to injection can create permeable paths in the tar zone, leading to water coning and excessive water production (Al-Kaabi et al., 1988).

The goal of this study was to investigate the adverse effects of the two most influential tarmat parameters i.e., tar viscosity and tar zone thickness on pressure behaviour, oil recovery and water saturation distribution during and after waterflooding. Another objective was to study the flow of tar due to aquifer expansion. A reservoir model representing the water, tar, and oil zones was simulated by a linear composite core. Experiments with different tar viscosities and tar zone thicknesses were conducted under controlled displacement flow rate, while maintaining all other experimental conditions as constant as possible.

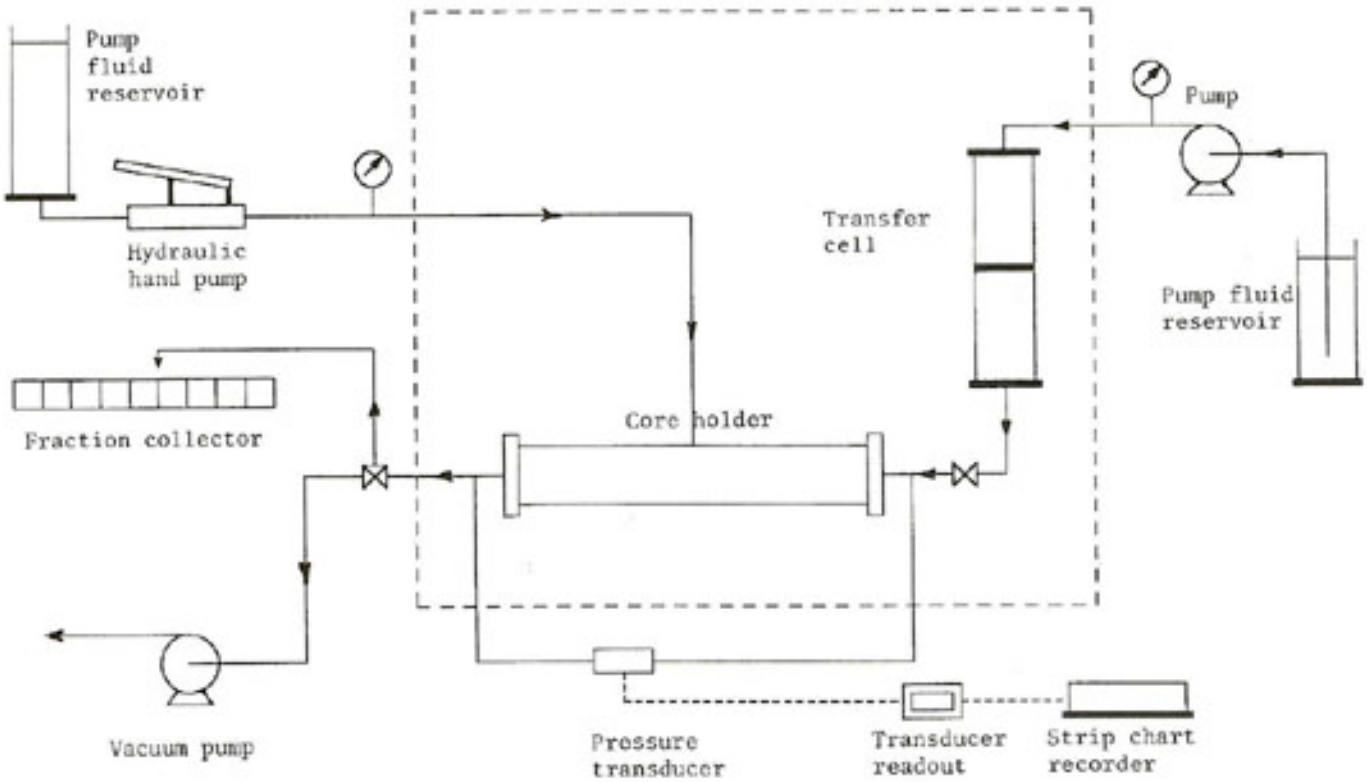

Fig. 2. Experimental apparatus.

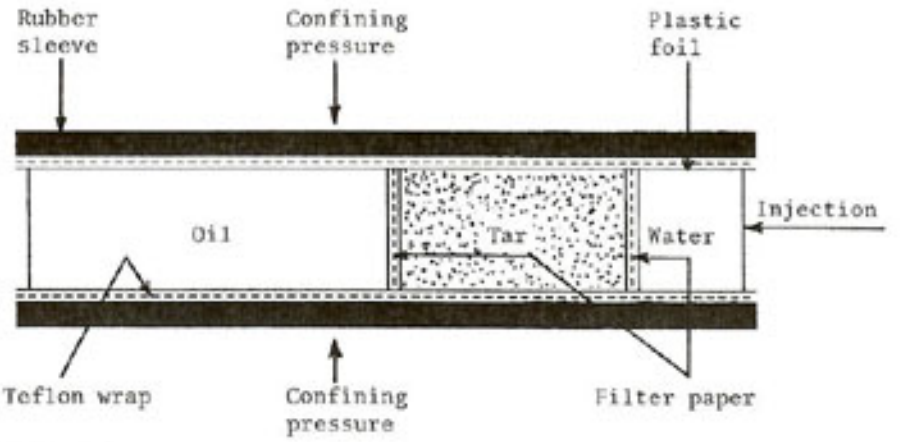

Fig. 3. Cross-sectional view of the linear composite core model.

Experimental apparatus

The experimental apparatus, shown schematically in Fig. 2, consists mainly of the fluid-injection system, displacement vessel and the fluid-collection system. The displacement vessel was a stainless steel, Hassler-type core holder designed for consolidated core samples up to 45 cm in length, 2.54 cm in diameter, and under confining pressures of up to 69 MPa. Details on the design and construction of the core holder as well as the components of the apparatus are found elsewhere (Ayub, 1989).

A reservoir volume element with sections of the water, tar, and oil zones is simulated by a linear composite core. The configuration of the composite core as it is loaded in the rubber sleeve is shown in Fig. 3.

Materials

Filtered kerosene and a solution of 1% KCl in distilled water were used to simulate the oleic and aqueous phases, respectively. The physical properties of these fluids are given in Table 1.

The tar phase was prepared from solutions of dead crude oil and asphalt. The properties of these two ingredients are also listed in Table 1. To prepare a batch of tar, a quantity of asphalt is first heated to reach a fluid stage; then a pre-estimated amount of crude oil is blended in to obtain a homogeneous solution of the desired viscosity. The batch is then allowed to cool down to room temperature, after which the tar viscosity is measured. The batch is then stored in a sealed container to be used for runs with the same tar viscosity.

Berea sandstone with an average porosity of 24% and absolute permeability of around 300 mD was used in all flooding experiments. All core plugs were fired at 900°C for 24 hours and

TABLE 1

Physical properties of fluids

Fluid	Property	
	Viscosity (mPa.s)	Density (g/cc)
Brine	0.820	0.980
Oil	1.131	0.764
	Distillation:	*Distillate*
Crude Oil	Temperature (°C)	(Vol%)
	225	8
	260	40
	316	80
	Solubility in CCl_4 (%)	99.5
	Flash Point, Open tag (°C)	27
	Gravity, at 25°C (ÅPI)	26.4
	Viscosity at 23°C (mPa.s)	243
Asphalt	Ductility at 25°C (cm)	2.5
	Flash point, C.O.C. (°C)	232
	Penetration, at 25°C 100 g, 5 s (0.1 mm)	15–25
	Loss on heating at 163°C 5 h, (%)	0.5
	Softening point, R & B (°C)	90.6
	Solubility in CCl_4 (%)	99.5
	Density (g/cc)	1.029

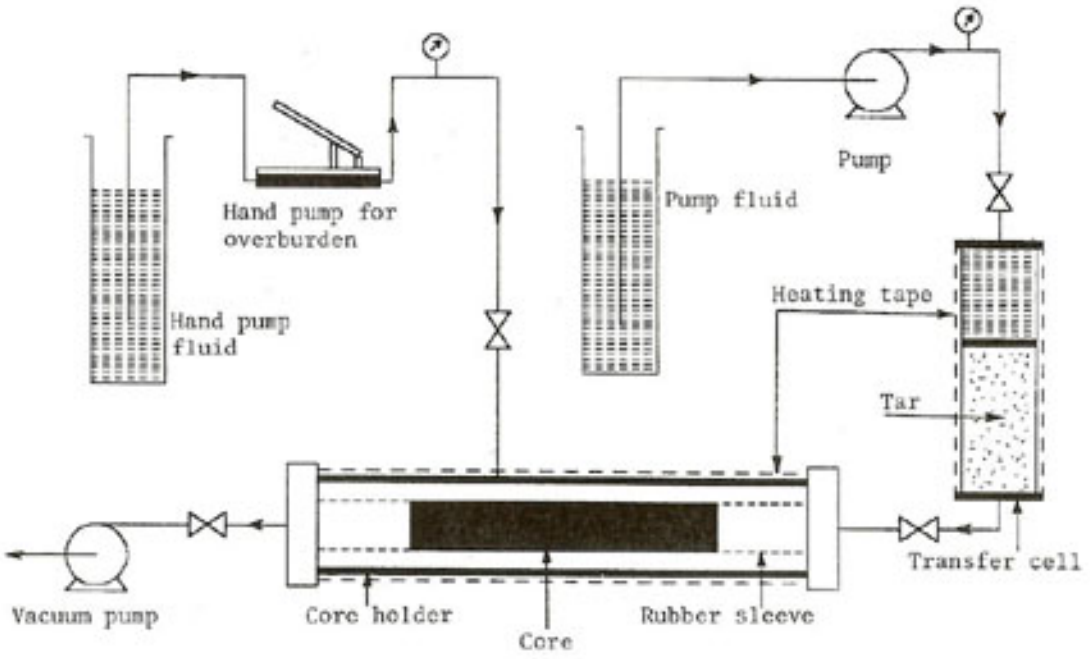

Fig. 4. Schematic of tar saturation set-up.

TABLE 2

Tar-zone pore volume as computed from water saturation and tar saturation separately

Run No	Length (cm)	Pore volume (cm^3)	
		Tar	Water
1	2.54	3.11	3.44
2	5.08	6.55	6.20
3	10.16	12.58	12.41
4	2.54	3.37	3.39
5	5.08	5.67	5.63
6	10.16	12.39	12.08
7	2.54	3.23	3.24
8	5.08	6.34	6.33
9	10.16	12.14	12.15
10	5.08	5.49	5.89
11	10.16	11.34	11.64
12	10.16	11.40	11.55
13	2.54	2.81	2.93

then flushed with isopropyl alcohol and dried in a vacuum oven before saturation with brine, oil or tar.

Saturation with tar was done at temperatures between 80° and 90°C using the core holder. Figure 4 shows a schematic of the tar-saturation set-up. After loading the tar cores and assembling the core holder, a confining pressure of 24.1 MPa is applied. Vacuum was then applied for several hours. Once the core holder and the transfer cell reach the desired temperature, injection of tar at very low rate is started. During tar injection, vacuum is applied continuously to help the tar move toward the production end. Injection is carried out in such a manner that the injection pressure is always considerably less than the confining pressure to avoid by-passing the core plugs. Vacuum is stopped immediately when tar appears at the outlet, but injection is continued until enough tar is produced to ensure 100% saturation. The core holder is then dismantled and the saturated cores are submerged in the same tar solution in a perfectly sealed container until ready to be used. Cores for experiments involving the same tar viscosity were saturated together. Pore volumes of the tar core plugs computed by tar saturation are compared with those computed by water saturation in Table 2. The data proves the success of the tar saturation process, as the water and tar volumes are reasonably close.

No connate-water saturation was intro-

duced in the tar zone for two reasons. First is the desire to standardize the connate-water saturation for all the experiments. This is necessary because the field connate-water saturation varies widely from one reservoir to another. The second reason is that the smaller the connate-water saturation, the more fingering induced. Therefore, a zero connate-water saturation represents extreme conditions of waterflooding of tar in tarmat reservoirs.

Experimental procedures

The saturated core plugs to be used in a displacement experiment were always arranged in the order shown in Fig. 3. Filter paper was placed between core plugs to allow better contact and capillary continuity. To ensure that no gap exists between the core plugs and the rubber sleeve, the cores were wrapped with a layer of plastic foil and a layer of teflon tape. The composite core was then loaded into the rubber sleeve, and the core holder was assembled in the experimental set-up as shown in Fig. 2.

To conduct a displacement run, the following steps were performed:

(1) A confining pressure of 13.8 MPa was applied in all displacement runs except for run 3 where a confining pressure of 20.7 MPa was applied because the injection pressure was expected to exceed 13.8 MPa due to the high tar-viscosity and thickness.

(2) Brine injection at a constant rate of 1.0 cc/min was then started and was continued until no more oil was produced.

(3) After a run was completed, the displacement vessel was dismantled and tar displacement was estimated carefully. Core plugs making up the oil and tar zones were then extracted for water-saturation measurement.

Results and discussions

A total of 13 tests were performed following the above described experimental procedure. All tests were performed at 24°C. The parameters varied, were the tar viscosity, the thickness of the tar zone, and the thickness of the oil zone. Table 3 lists the experimental variables for these runs. All thirteen runs displayed very similar trends as far as the pressure variation, tar phase movement, variation of average-water saturation in oil and tar zones, and the oil recovery before and after water breakthrough. The magnitude of these trends differs, though, from one run to another.

TABLE 3

Experimental variables

Run	Tar viscosity* (mPa s)	Tar density* (g/m^3)	Zone length (cm)		
			Water	Tar	Oil
1	21,000	0.930	2.54	2.54	10.16
2	21,000	0.930	2.54	5.08	38.10
3	21,000	0.930	2.54	10.16	15.24
4	10,000	0.924	2.54	2.54	10.16
5	10,000	0.924	2.54	5.08	38.10
6	10,000	0.924	2.54	10.16	15.24
7	5,000	0.919	2.54	2.54	10.16
8	5,000	0.919	2.54	5.08	38.10
9	5,000	0.919	2.54	10.16	15.24
10	15,000	0.927	2.54	5.08	33.02
11	15,000	0.927	2.54	10.16	20.32
12	15,000	0.927	2.54	10.16	33.02
13	15,000	0.927	2.54	2.54	22.86

*at 24°C.

Pressure behaviour

An initial period of sharp pressure build-up at the injection point followed by a gradual pressure decline was always noticed. Figure 5 shows a typical variation of inlet pressure versus volume of brine injected in tar zone pore-volumes (TZPV). The sharp build-up is believed to be caused by the initial accumulation of water and its very slow initial advance through the tar zone. This is due to the extremely low mobility of tar. Consequently, no oil production during the initial period of injection was observed since tar displacement was negligible.

The maximum-pressure levels varied with

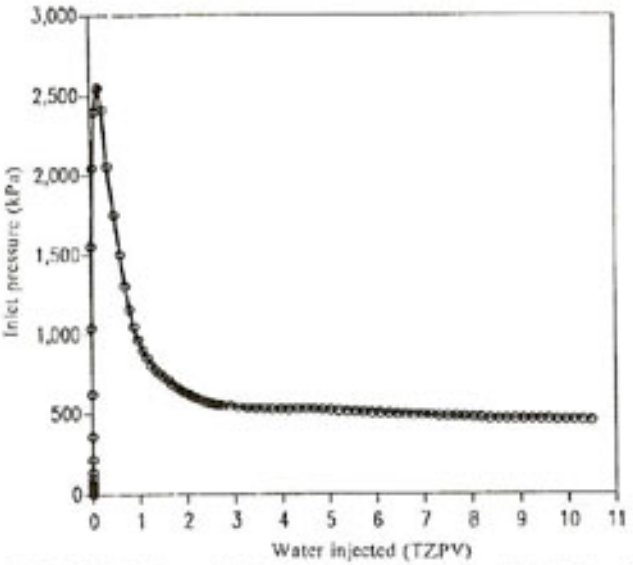

Fig. 5. Variation of inlet pressure with water injection for run 5.

the tar viscosity and with the thickness of the tar zone. That is, a higher pressure was obtained with a higher tar viscosity or with a thicker tar zone. The maximum pressure attained during each run is listed in Table 4 and is plotted versus tar zone thickness in Fig. 6 and versus tar viscosity in Fig. 7. Eventhough the data in these figures is limited, one can observe that:

$$\partial^2 P_{max}/\partial \mu_t^2 \leqslant 0 \text{ and } \partial^2 P_{max}/\partial h_t^2 \geqslant 0$$

It is also observed that these derivatives approach zero at low tar viscosities or small tar-zone thicknesses.

Table 4 also provides a comparison between the time required to reach the maximum pressure (T_p) and the time of water breakthrough into the oil (T_b). T_b is always higher than T_p, except in run 4, where it might be due to some unavoidable experimental error. The time required to start the oil production (T_i) for each displacement run is also listed in Table 4. Oil production was noticed before T_p in most of the runs.

The extremely high viscosity-ratios involved in the displacement experiments of this study make the displacement of tar by water occur at highly unfavourable mobility-ratios. Therefore, the displacement front cannot be stabilized as required by Buckley and Leverett (1942) which causes appearance of viscous fingers (Perkins et al., 1969).

The initiation of viscous finger(s) is presumed to be triggered by instabilities at the interface between the displacing fluid and the displaced fluid. Unstabilized flow causes these fingers to propagate and grow through the displaced phase (Perkins et al., 1969, Vossoughi

TABLE 4

Experimental results

Run No	T_i (min)	T_p (min)	T_b (min)	P_{max} (kPa)	Q_{it} (TZPV)	Q_{io} (OZPV)	$\bar{S}_w$		R (% OOIP)
							Tar zone	Oil zone	
1	9.50	9.00	16.00	1186	0.10	0.71	3.2	17.3	37.7
2	8.00	7.20	32.00	3344	0.11	0.63	10.7	45.4	57.5
3	8.00	15.00	20.50	15265	0.21	0.67	17.5	29.9	65.2
4	4.00	10.00	9.00	354	1.72	0.50	5.9	37.7	45.8
5	6.50	7.60	29.50	2551	0.18	0.57	5.3	34.8	56.4
6	5.00	13.20	17.50	9687	0.29	0.51	8.1	36.9	51.4
7	5.00	8.30	11.50	312	0.68	0.52	6.2	43.3	50.1
8	4.75	8.00	30.00	1655	0.18	0.59	7.9	45.6	57.1
9	6.75	14.88	18.00	5350	0.27	0.56	8.2	43.6	54.6
10	6.50	9.80	25.50	2965	0.47	0.57	9.1	46.5	57.1
11	6.00	11.00	20.50	13514	0.17	0.56	8.8	38.8	54.9
12	6.00	16.50	27.00	12755	0.62	0.57	15.8	40.4	56.9
13	4.50	7.60	19.00	1117	0.39	0.56	10.7	43.7	55.6

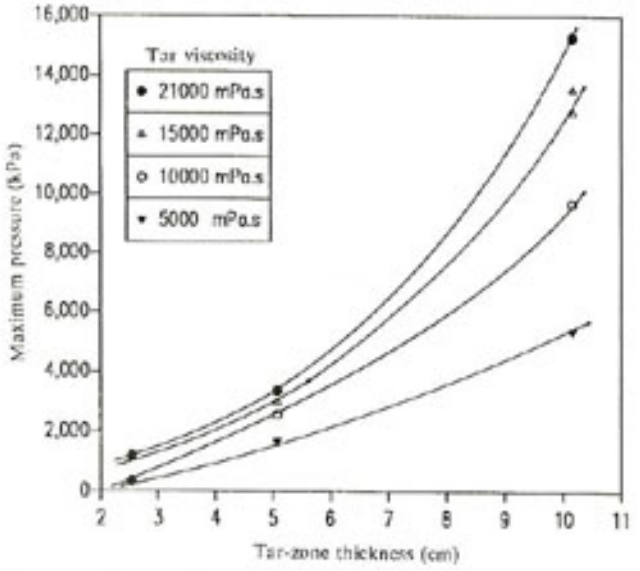

Fig. 6. Effect of tar-zone thickness on maximum inlet pressure.

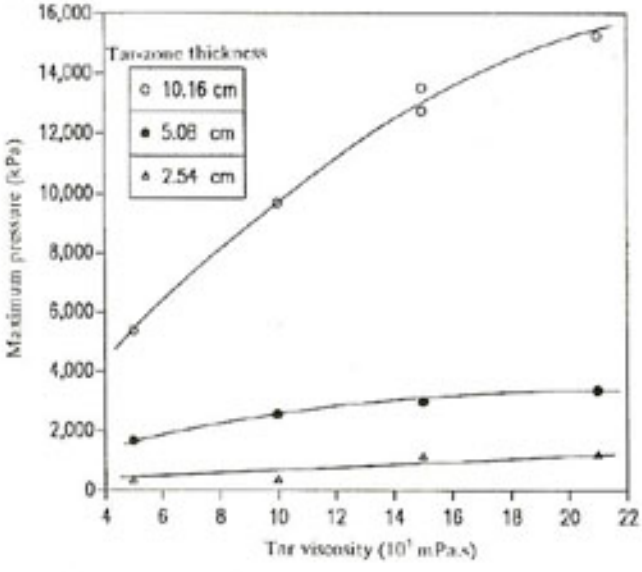

Fig. 7. Effect of tar viscosity on maximum inlet pressure.

et al., 1982). The presume is, in this study, that the growth of viscous fingers coincides with the initial period of pressure build-up in the core. No significant growth in the size of a finger(s) occurs after water breaks through the tar zone, due to the high viscosity of tar. This fingering theory for the invasion of tar by water and for the displacement of oil by water thereafter will be further discussed later.

Regression analysis produced Eq. 1 as the best fit to the data of Figs. 6 and 7.

$$P_{max} = 1.71\times10^{-3}\mu_t h_t^2 - 3.28\times10^{-8}(\mu_t h_t)^2 \quad (1)$$

Although Eq. 1 has no theoretical basis, it does predict the disappearance of the pressure peak at low tar-viscosities. This should be the case as the tar phase behaves more like a Newtonian fluid under these conditions.

Average water saturation

The average water-saturations in the oil and tar zones after flooding were obtained by core extraction. Table 4 gives these average water-saturations in both zones for all thirteen runs.

Tar zone

The data of Table 4 shows no correlation between $\bar{S}_{wt}$ and either tar viscosity or thickness. However, a fair correlation exists between $\bar{S}_{wt}$ and the total resistance to flow $\mu_t h_t$ as depicted by the tar-zone data of Fig. 8.

Eventhough, the final water-saturation profile in the tar zone, as determined in some runs with long enough tar zones, displayed the usual shape, i.e., decreasing in the direction of flow, an increase in $\bar{S}_{wt}$ with larger values of $\mu_t h_t$ is

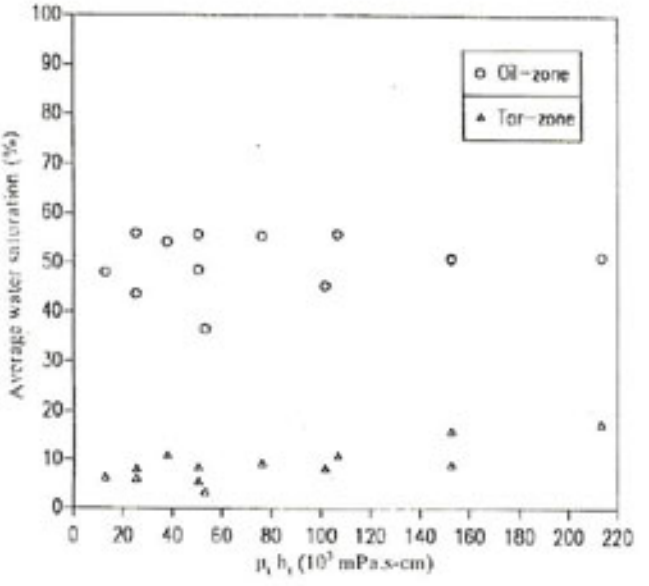

Fig. 8. Effect of tar-zone viscosity-thickness product on post-flooding average water saturation.

contrary to what is observed in immiscible fluid-displacement at ordinary viscosity ratios. One can only speculate that the shape and size gradation of the water finger(s) are a primary cause of this phenomenon.

Oil zone

The final water-saturation profile in the oil zone at the end of run 10 is shown in Fig. 9. The shape of this profile was found to be typical in the experiments of this study. This saturation distribution is contrary to what is usually observed in regular water/oil displacement tests, i.e., the saturation decreases in the direction of flow. It can be explained by the notion that the water finger(s) which develop within the tar zone gradually stabilize and ultimately disperse as they move through the oil zone.

This behaviour was reported by Perkins and Johnston in 1969. Some of their data indicated that viscous fingers which formed at the entrance of a glass-bead pack tended to disperse and deteriorate into a zone of graded saturation as they moved through the pack. Similar results were reported for Berea sandstone from interpretations of X-ray shadowgraphs.

The dispersion of fingers suggests that capillary forces may oppose the development of fingers and may dampen their propagation in strongly water-wet porous media. It also indicates restabilization of the displacement once the oil/water viscosity ratio is brought down to normal levels. Because of the nature of the porous media used in this study, strongly water-wet Berea sandstone, the wettability plays a role opposite to the viscosity effect. It is expected that since the viscosity ratio investigated is very large, the effect of change of wettability will be minimal compared to the viscosity effect.

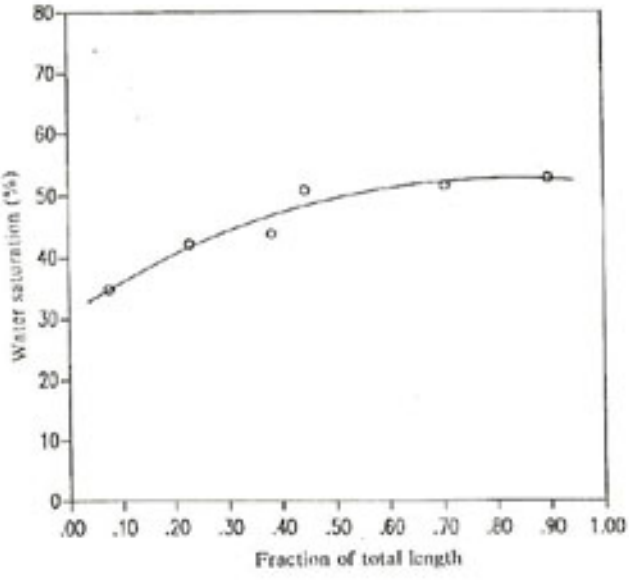

Fig. 9. Post-flooding water saturation profile in the oil-zone, run 10.

The above arguments provide an explanation for the variation in the post-flooding average water-saturation in the oil zone, $\bar{S}_{wo}$, with tar-zone properties. Since a higher resistance leads to fewer fingers, the final volume of these fingers after they disperse in the oil zone will be smaller. Thus, $\bar{S}_{wo}$ decreases with increase in $\mu_t h_t$. Except for a few outliers, most of the oil-zone data points of Fig. 8 confirm this trend.

Oil recovery

A typical history of oil recovery (% OOIP) versus volume of brine injected (OZPV), Q_{io}, is shown in Fig. 10. All runs displayed similar trends for oil recovery differing only in magnitude. The final oil-recovery for each of the thirteen runs is listed in Table 4 as well as the values of Q_{io} corresponding to these recoveries. It should be pointed out that the breakthrough recovery is almost equal to the final recovery and a negligible amount of oil was produced after breakthrough in all runs.

Two interesting findings are made from the data of Table 4. First, since the final recovery is equal to the breakthrough recovery, this indicates piston-like displacement within the contacted pore-space of the oil zone. It also indicates that the water-saturation profile in the oil zone does not change beyond breakthrough. The second finding is that Q_{io} at the final recovery varies over a small range with

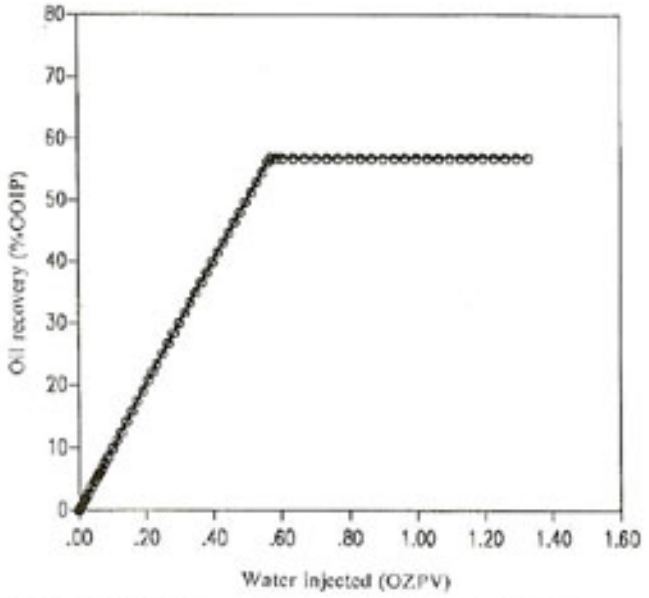

Fig. 10. Variation of oil recovery with water injection, run 12.

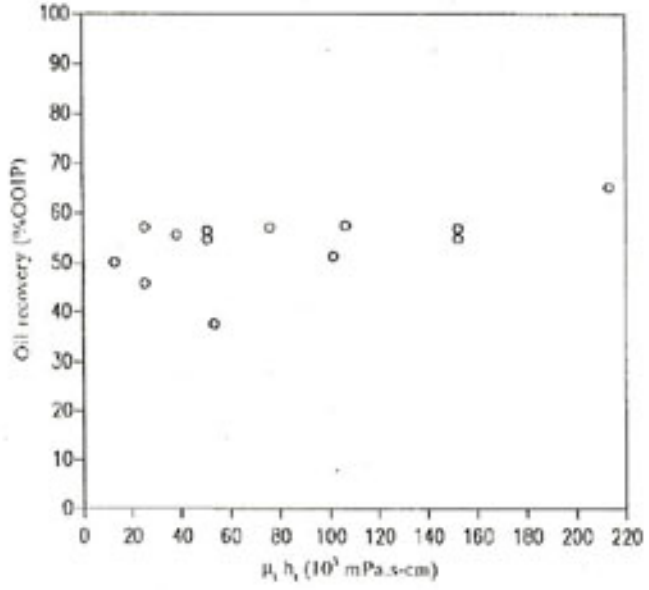

Fig. 11. Effect of tar-zone viscosity-thickness product on final oil recovery.

an average of 0.58 and standard deviation of 0.06. It can be concluded that an approximate average value $Q_{io}=0.58$ is required to get the maximum oil-recovery from this type of flooding experiments. As with $\bar{S}_{wo}$, the final recovery displayed a slight decrease with increase in $\mu_t h_t$ as shown in Fig. 11.

Dynamic behaviour of the tar phase

Tar movement

All of the runs displayed a significant tar movement. Under water encroachment, the tar always invaded the oil zone as could be clearly detected by core inspection after flooding. The relative movement depended naturally on the tar-phase viscosity and thickness. The total advance of the tar/oil interface, as a fraction of the original tar zone thickness, varied between 0.4 and 0.6.

The tar/oil interface maintained its distinct, planar shape but with a slight reduction in the colour contrast between the two fluids. This indicated near total displacement of oil by tar with a small degree of mixing. This is in contrast with displacement of tar by water at the upstream end of the tar zone which was dominated by viscous fingers. Before water breakthrough, only oil was produced from the core holder, and tar was never produced at any phase of the experiments.

Effective permeability to water

Since the viscosity of oil is negligible compared to that of the tar, the bulk of the overall

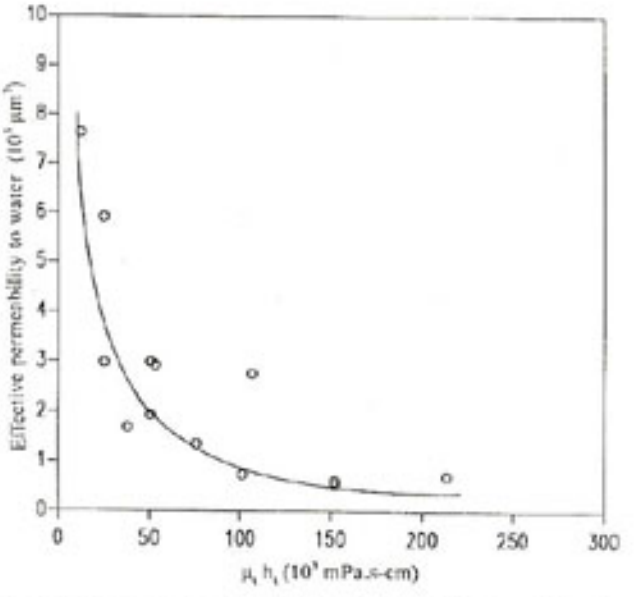

Fig. 12. Effect of tar-zone viscosity-thickness product on post-flooding effective permeability to water in the tar zone.

pressure-drop across the composite core took place within the tar zone. Hence, the effective permeability to water in the tar zone, K_{wt}, can be computed assuming a uniform water saturation in the tar zone. This simplifying assumption is warranted given the relatively small thickness of the tar zone.

In Fig. 12, K_{wt}, measured at the end of flooding, is plotted versus $\mu_t h_t$ for all runs. The figure reveals much sensitivity of K_{wt} to $\mu_t h_t$ at low values of this parameter. Non-linear regression analysis of the data of Fig. 12 produced the following best fit:

$$K_{wt} = 27.09 - 2.225 \ln \mu_t h_t \qquad (2)$$

Conclusions

The results and theoretical discussions presented in this study lead to the following conclusions:

(1) Pressure behaviour, average water saturation both in the tar and oil zones, and oil recovery indicate the development of viscous fingers.

(2) The size of the water finger(s) in the oil zone increases towards the outlet. This phenomenon was deduced from water-saturation profiles in the oil zone.

(3) Reduction in oil recovery against total resistance to flow is not significant.

(4) Average water saturation increases in the tar zone with total resistance to flow.

(5) The mechanism by which the water invades the tar zone displayed the same characteristics for all tar viscosities and thicknesses.

(6) The effective permeability to water in the tar zone decreases with increase in total resistance to flow, and shows rapid decline at low values of $\mu_t h_t$.

Acknowledgements

Work involved in this study was performed as part of project No. AR/7/152 funded by King Abdul-Aziz City for Science and Technology, Riyadh, Saudi Arabia. The authors wish to thank KACST for all its financial and technical support.

Notations

h_t	tar zone thickness (cm)
K_{wt}	effective permeability to water in tar zone (mD)
OOIP	original oil in place (cm^3)
OZPV	oil zone pore volume (cm^3)
P_{max}	maximum pressure (kPa)
Q_{io}	volume of brine injected, oil-zone pore volumes
Q_{it}	volume of brine injected, tar-zone pore volumes
R	oil recovery, fraction of OOIP
S_w	average water saturation, percent or fraction
S_{wo}	average water saturation in the oil zone, percent or fraction
S_{wt}	average water saturation in the tar zone, percent or fraction
T_b	water breakthrough time (min)
T_i	time of first oil production (min)
T_p	time of maximum pressure (min)
TZPV	tar zone pore volume (cm^3)
μ_t	tar viscosity (mPa s)

References

Al-Kaabi, A.U., Menouar, H., Al-Marhoun, M.A and Al-Hashim, H., 1988. Bottom water drive in tarmat reservoirs. SPE Res. Eng., (May): 395–400.

Ayub, M., 1989. The effects of tar viscosity and thickness on oil recovery in a tarmat reservoir model. M.S. Thesis, King Fahd University of Petroleum & Minerals, Dhaharan, Saudi Arabia, (June 1989).

Bashbush, J.L., Savage, W.K., Nagai, R.B., Gimoto, T., Wakamiya, J. and Takizawa, H., 1983. A reservoir optimization study, El-Bunduq field, Abu Dhabi, Qatar. SPE 11481, presented at the 3rd SPE Middle East Oil Show, Manama, Bahrain, (March 1983).

Buckley, S.E., Leverett, M.C., 1942. Mechanism of fluid displacement in sands. Trans. AIME 146: 107–16.

Hirschberg, A., 1988. Role of asphaltenes in compositional grading of a reservoir's fluid column. J. Pet. Technol., (Jan.): 89–94.

Moor, L.V., 1984. Significance, classification of asphaltic material in petroleum exploration. Oil & Gas Journal, (Oct.): 109–112.

Osman, M.E., 1985. An approach to predict tarmat breakdown in Minagish reservoir in Kuwait. J.Pet. Technol., (Nov.): 2071–2075.

Perkins, T.K., Johnston, O.C., 1969. A study of immiscible fingering in linear models. SPE J., (March): 39–46.

Richardson, J.G., Harris, D.G., Rossen, R.H. and Van Hee, G., 1978. The effect of small, discontinuous shales on oil recovery. J. Pet. Technol., (Nov.): 1531–37.

Vossoughi, S., Smith, J.E., Green, D.W. and Willhite, G.P., 1982. A new method to simulate the effects of viscous fingering on miscible displacement processes in porous media. SPE 10970, presented at the 57th Annual Fall Technical Conference and Exhibition of SPE of AIME, New Orleans, LA., (Sept. 26–29, 1982).